Laser interaction with Br-GaAs(110): Etching and atomic desorption

B. Y. Han and J. H. Weaver
Department of Materials Science and Chemical Engineering, University of Minnesota, Minneapolis, Minnesota 55455
(Received 18 March 1998; revised manuscript received 18 May 1998)

Scanning tunneling microscopy was used to investigate changes in the surface morphology of GaAs(110) induced by 2.3 eV photons from a Nd:YAG (yttrium aluminum garnet) laser. For clean surfaces, irradiation caused minimal changes. For surfaces decorated by islands of Br, however, irradiation created monolayer pits whose shapes reflected the chemisorption structures. The desorption yield followed a square law for low laser intensities ($F \leqslant 13.5$ mJ cm^{-2}) due to photochemical conversion of GaBr to volatile $GaBr_3$. 70–80% of the etch pits were composed of pair vacancies due to removal of gallium as $GaBr_3$ and arsenic as molecular As. These photochemical processes are enhanced by photothermal effects, even in the low intensity regime. Pit growth after Br depletion occurs via laser-induced desorption of Ga and As from pit edges. Growth along [110] is favored, reflecting the contrast in surface bonding strengths. Atomic desorption is initiated by electronic excitations, probably involving multiple electronic excitations. The yield varies as $F^{(3-3.5)}$. As with photoetching, it increases with base temperature. Both photoetching and laser-induced desorption result in stoichiometric removal, and the top layer can be removed by extended irradiation. [S0163-1829(98)10139-X]

I. INTRODUCTION

Laser-enhanced dry etching of semiconductors has attracted considerable interest due to its potential in microfabrication.[1] Important work has focused on photochemical and thermal effects underlying the etching processes.[2–7] In photochemically enhanced etching, free-charge carriers generated by light absorption directly participate in surface reactions. In photothermal etching, carrier relaxation and recombination processes convert the absorbed photon energy to lattice heating that activates etching. Here, we examine the interplay between photochemical and photothermal etching for Br-decorated GaAs(110) as a function of laser intensity, F, and substrate base temperature. This etching is photochemical for laser pulse intensities $F \leqslant 13.5$ mJ cm^{-2} under our experimental conditions but direct photothermal effects contribute at higher intensities. Increasing the base temperature enhances photochemical reactions. Photoetching of ideal terraces produces irregular, single-layer-deep defects that reflect the Br chemisorption structures. We also identify a predominant pairwise removal of Ga and As from surface lattice sites, similar to thermal etching under low halogen flux and/or coverage conditions.

Laser-solid interactions can result in atom desorption from defect sites for irradiation intensities below the ablation threshold, even for clean surfaces.[8–10] The observation of distinguishable components in the emission yield indicates emission from different defect types (adatoms, steps, vacancies). Here, we show that irradiation after pitting causes Ga and As desorption from pit edges. The pits grow preferentially along [110] due to bonding strengths at different step sites and long stripes of exposed second layers are produced. The yield reflects the density of atoms at pit boundaries and their step types and it follows power law dependence on laser intensity. Analysis based on the yield and the laser intensity suggests an active role by multiple electronic excitations.

II. EXPERIMENTAL

Scanning tunneling microscopy was used to characterize the GaAs(110) surface morphology during material removal. All experiments were done at pressures under 1×10^{-10} Torr. Starting surfaces were obtained by cleaving p-type GaAs crystals (Zn-doped at 1×10^{18} cm^{-3}; MCP Wafer Technology, Ltd., U.K.; initial dimensions $\sim 3 \times 3 \times 10$ mm^3). Typical surfaces had terraces with widths of 3000–5000 Å, separated by kinked $[\bar{1}10]$ or $[1\bar{1}n]$ steps, and defect densities below 1×10^{12} cm^{-2}, mostly in the form of point defects or adatoms.

Freshly cleaved surfaces were exposed at 300 K to molecular Br_2 from a solid-state electrochemical cell[11] to give an initial coverage of 0.04–0.25 ML [1 ML $= 8.84 \times 10^{14}$ cm^{-2}, the planar density of GaAs(110)]. Subsequent laser irradiation reduced the Br surface concentration and produced pits. The base temperature of the sample could be adjusted in the range 300–800 K by tungsten filament heating, using a thermal couple to monitor the temperature. After each reaction/irradiation step, the sample was transferred to the scanning tunneling microscope (STM) stage and images were recorded at room temperature (tip voltage 1.8–3.2 V, current 0.1–0.2 nA). All STM images displayed here reflect the As-sublattice (occupied-state images). The Br coverages, the etch pit densities, and the total pit areas were determined by direct counting from such images.[12,13]

A frequency doubled Nd:YAG (yttrium aluminum garnet) laser emitting 2.3 eV photons (532 nm) was coupled to the measurement chamber through a quartz window. The laser was Q-switched with a pulse duration of ~ 6 ns and pulse energy up to 200 mJ. It was usually operated in a single shot mode or with a repetition frequency of 10 Hz. The beam was incident upon the sample at normal incidence with the electric field vector **E** more than 90% polarized parallel to [001] unless otherwise specified. To ensure beam uniformity, we used a 1-mm aperture in the laser cavity to transmit only the TEM_{00} mode. A dispersive lens was used to spread the beam to obtain a sufficiently large area on the sample that was homogeneously irradiated. A photodiode with $\sim 1/4$ mm aperture was placed at the sample position to determine the beam profile after attenuation using appropriate neutral density filters. Under our experimental configuration, the beam

profile was approximately Gaussian (full width at half maximum≈5 mm) plus a ''hot cap'' of ~1.5 mm diam at the beam center. The intensity in this ''hot cap'' was uniform to within ~5% and it was this part of the sample that was selected for STM imaging. The pulse energy was measured by a laser power meter (SCIENTECH Astral AC2501) and shot-to-shot variation was ~4% after a 20 min warm-up period. The pulse energy intensity (laser intensity) was maintained at $F_0 = 45$ mJ cm^{-2}. Beam intensities were reduced by inserting neutral density filters. To check reproducibility, the irradiation/imaging sequence for each intensity setting was performed at least twice. For each, 2–3 positions on the sample surface, ~0.5 mm apart, were chosen for imaging to verify uniformity of irradiation.

III. RESULTS AND DISCUSSION

A. Etch pit creation in photoetching

This section focuses on etch pit creation on terraces with a low concentration of Br distributed in chemisorption islands. As a check, we first irradiated a clean surface with 10^4 pulses at 35 mJ cm^{-2}. The resulting surface had essentially the same defect density as the starting surface, $\leqslant 1 \times 10^{12}$ cm^{-2}, although the total pit area increased slightly due to growth of existing pits (see Sec. III C). We conclude that laser-induced terrace pit initiation is minimal under our conditions.

Figure 1(a) was obtained after exposure at 300 K to produce 0.04 ML Br. Most Br adatoms are bonded to Ga in island structures, though there are some brighter features within the islands that reflect Br-As bonding. Island I crosses 12 rows (68 Å) along [001] but has an average width of only 3–4 unit cells (12–16 Å) along [110]. Island II has an aspect ratio of about 1 and is derived from about 25 adatoms. This tendency to form islands reflects an attractive adatom-adatom interaction[12,14] which favors alignment along [001]. Kinetic constraints associated with Br condensation at room temperature result in a range of sizes, including those derived from only a few adatoms.

Terrace pitting occurred when the surface in Fig. 1(a) was irradiated, as in Figs. 1(b) and 1(c) for 2×10^3 pulses at 35 mJ cm^{-2}. At this stage, about 3% of the top-layer GaAs(110) has been removed, and the Br concentration decreased to less than 0.005 ML. In occupied-state images, the end of a vacancy row appears brighter if it is As terminated and dimmer if Ga terminated.[12] Conclusions regarding the bounding species of vacancy rows were verified by dual-bias imaging. $P1$ corresponds to a Ga-As vacancy pair since it is 8 Å long with ends that have different appearances. $P2$ reflects a Ga-As-Ga trivacancy, and both ends appear bright. $P4$ reveals two missing Ga-As pairs. It is bounded by an As atom at the upper end and a Ga atom with a Br adatom atop at the lower end. $P5$ highlights a pit formed by three Ga-As vacancy pairs on the left row and two pairs on the right row.

Extended pits are also produced by photoetching. Pit $P3$ crosses six rows. This suggests that it formed from a structure like island I. Its irregularity may indicate that more than one initiation site was involved. Counting from the lower left of $P3$, the number of pairs removed in each row is 2, 2, 1, 1, 2, and 1. Pits elongated along [001] like this are not observed after thermal etching where the Br diffusion length is larger. Here, the Br diffusion length during the pulse is only a few lattice constants, although attachment and detachment at island boundaries is possible.[15] For this reason, etch pit profiles tend to reflect the chemisorption footprint. Pit $P6$ reflects removal of about 15 Ga-As pairs. It probably developed from an island like II.

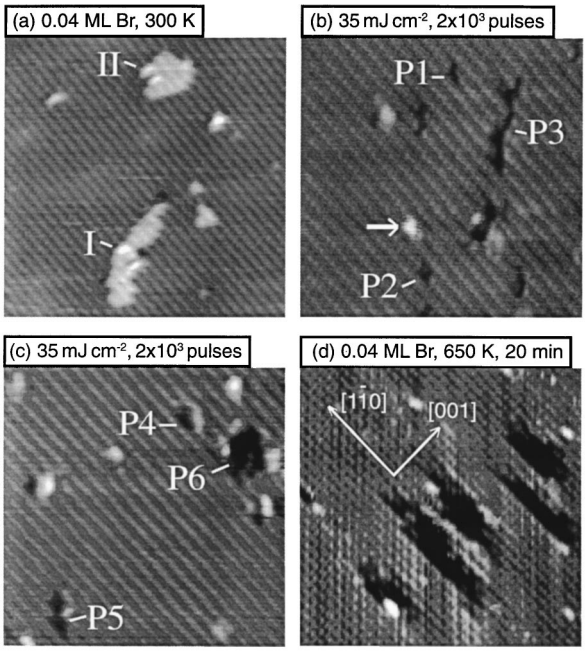

FIG. 1. STM images showing terrace pits produced by laser and thermal etching of Br-GaAs(110). (a) A surface with 0.04 ML Br accumulated at 300 K showing chemisorption islands. Islands I and II represent dozens of adatoms. Images (b) and (c) show single-layer deep pits like $P1$ and $P2$ that are confined to 1–2 rows. Pits 4 and 5 reveal two and three vacancy pairs. Pits $P3$ and $P6$ are substantially larger and would have been produced by structures like islands I and II, respectively. Image (d) was obtained after heating a surface like 1(a) to 650 K for 20 min. Thermal etching produced larger elongated pits with straight edges. The amount of etching in (d) is greater because Br is consumed via GaBr desorption rather than $GaBr_3$ desorption. [(a) and (d) 200×200 Å^2, (b) and (c) 140×140 Å^2]

Analysis of dozens of images shows that 70–80 % of the pits were composed of pair vacancies. Moreover, the pit boundaries are made of equal numbers of Ga and As, both for low Br coverage, Fig. 1, and for more extensive etching with higher initial Br coverages. This indicates stoichiometric removal under our experimental conditions. Such pairwise removal of Ga and As has been observed in thermal etching when dosed surfaces are heated to 650 K.[12] Since the species that can desorb are GaBr, $GaBr_3$, and molecular As (as discussed below), a plausible scenario for pairwise removal is that gallium-bromide desorption is accompanied by As ejection onto the terrace. This adsorbed As atom diffuses until it can form volatile As_2 (or As_4) and desorb. The presence of adsorbed As is supported by the observation of features such as that identified by the arrow in Fig. 1(b). This feature is 1.5–1.8 Å high (occupied state image) and is bonded to a Ga atom. Such moieties have previously been observed after thermal etching and were attributed to As.[12]

Comparison of photochemical and direct thermal etching can be made through Figs. 1(b)–1(d). To obtain Fig. 1(d), we accumulated 0.04 ML Br and then heated to 650 K for 20 min. In this kind of thermal regime, pits are created by $GaBr_3$ desorption and then pits grow preferentially along the zigzag row direction by GaBr desorption. Pit growth along the row direction involves nominally twofold-coordinated substrate atoms whereas growth across rows involves removal of threefold-coordinated atoms. When the initial concentration of Br is low, as for Fig. 1(d), etching should favor [110] growth via GaBr desorption since $GaBr_3$ precursors would be formed less frequently. Analysis shows that the etching evident in Fig. 1(d) resulted in ~0.08 ML removal, more than twice as high as in photoetching. This reflects a different partitioning between the desorbing $GaBr_3$ and GaBr species (discussed in Sec. III B).

B. Laser-etching of Br-GaAs(110): Photochemical versus photothermal

This section focuses on the dependence of photoetching on laser intensity and substrate temperature. Previously, we showed that etch pits were generated on Br-GaAs(110) after extensive irradiation with low-intensity (3 mJ cm^{-2}) laser pulses.[15] Since the peak temperature achieved under those conditions was only ~20 K above ambient, and therefore well below that needed for thermal etching, ~500 K,[13] it was argued that pitting was caused by substrate-mediated charge transfer. For the chemisorbed initial state, we can infer participation by Br-Ga antibonding levels derived in part from the Br $4p$. This level is above the conduction-band minimum while the Br-As level is ~0.28 eV above the valence-band edge.[16] The Br-Ga and Br-As bonding levels are 3.2 and 4.7 eV below the valence-band edge and are inaccessible for 2.3 eV photons. A series of intermediate configurations must be accessed as the adsorbate Ga complex evolves from GaBr(a) to $GaBr_3$(a), which can desorb with a small barrier. Here, we investigate the interplay of such (nearly pure) photochemical etching with photothermal processes that contribute to nuclear motion.

Figure 2(a) shows a STM micrograph of a typical starting surface with 0.25 ML Br. Exposure at 300 K was followed by heating to 400 K for 20 min to enhance ordering. The bright features reflect Br bonded to As sites.[12,13] They appear as chains elongated along [001] or groups of chains with mixed $2\times1/c(2\times2)$ symmetry. Within the islands, the Ga sites and half of the As sites are Br terminated, as depicted at the bottom of Fig. 2.

Figures 2(b) and 2(c) were obtained after irradiation with 100 and 200 pulses at a base temperature of 350 K with 45 mJ cm^{-2}. The number of adatom features has decreased as single-layer-deep etch pits have been formed. In Fig. 2(b), the pits accounted for 0.07 ML (density $\sim1.4\times10^{13}$ cm^{-2}) and typical pits extend over only a few unit cells. Between Figs. 2(a) and 2(b), the Br concentration was reduced from 0.25 to 0.16 ML. After 200 pulses, the Br concentration was reduced to 0.06 ML while the pit area was 0.15 ML (density 1×10^{13} cm^{-2}). The expansion and overlap of adjacent pits accounts for the larger area and smaller density. Increasing the number of pulses to 600 increased the pit area to 0.2 ML (density 6×10^{12} cm^{-2}) as the Br concentration became negligible. Subsequent pit growth depended entirely on laser-induced atomic desorption, and this was a lower yield process.

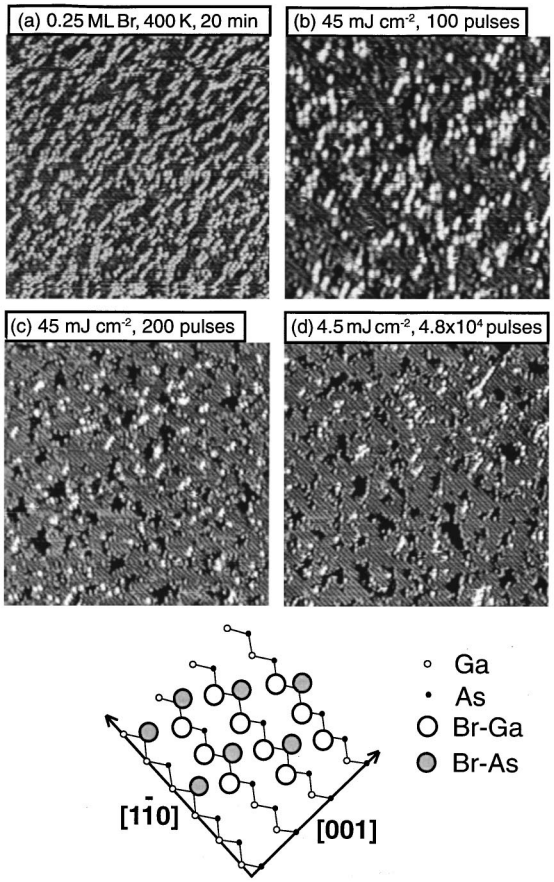

FIG. 2. Image (a) was obtained for a surface with 0.25 ML of Br that was heated to 400 K for 20 min to enhance ordering. The bright features reflect Br bonded to As. All Ga sites and half of the As sites are Br terminated within groups of chains, as depicted at the bottom. These chains are elongated along [001]. Images (b) and (c) show pit formation. 90% of the Br is lost through $GaBr_3$ desorption. Image (d) shows a morphology equivalent to (c) after irradiation at lower power but more pulses. Morphologies like (c) and (d) can be reached with intermediate power settings by varying the number of pulses. [(a), (c), and (d) 400×400 $Å^2$; (b) 250×250 $Å^2$]

In experiments like those represented by Fig. 2, we separately varied the laser intensity, the number of pulses, and the substrate base temperature T_0 to obtain images until the Br coverage was reduced from the initial coverage of 0.25 ML to 0.06 ML.[17] This allowed us to determine the number of substrate atoms removed per cm^2 per pulse, the *desorption yield*. This procedure is justified because essentially the same morphology can be achieved for different laser intensities simply by varying the number of laser pulses. Figures 2(c) and 2(d) demonstrate this morphology for samples irradiated at 350 K with 200 pulses at F_0 and 48 000 pulses at $0.1F_0$ where $F_0=45$ mJ cm^{-2}. Both have pit areas ~15%, densities $\sim1\times10^{13}$ cm^{-2}, and residual Br ~0.06 ML. We note that the morphology is not determined solely by dose, the energy intensity of each pulse multiplied by the number of pulses. Instead, it depends sensitively on the pulse intensity, as discussed in more detail below.

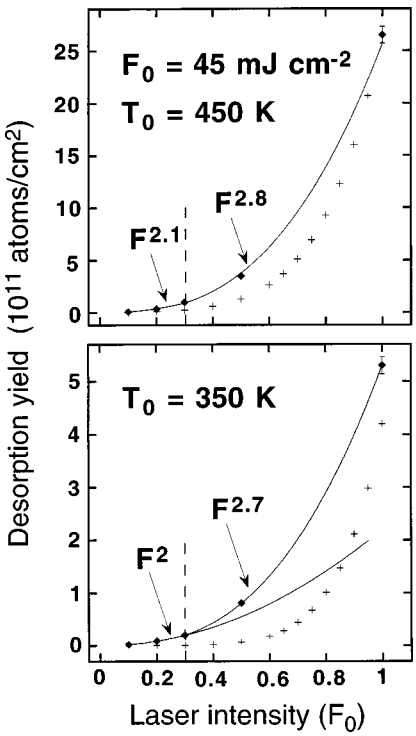

FIG. 3. Desorption yield as a function of laser intensity F for base temperatures of 350 and 450 K. F_0 is 45 mJ cm^{-2}. The desorption yield at 350 K increases as F^2 due to a photochemical conversion of GaBr (a) to $GaBr_3$ (a) which desorbs. Above $0.3F_0$, the yield increases as $F^{2.7}$ due to thermal contributions. The yields at 450 K are 4–5 times larger than at 350 K at the same intensity. The (+) signs represent the maximum thermal etching contribution as derived from the Arrhenius relation and normalized to the yield at F_0 and 450 K. This greatly overestimates the direct thermal contributions but still shows that the thermal etching is small at low power (below $\sim$13.5 mJ cm^{-2}).

Figure 3 shows the desorption yield for laser intensities of $0.1-1.0F_0$ at base temperatures of 350 and 450 K. The yield varies from 2.2×10^9 atom-pulse^{-1} cm^{-2} for $0.1F_0$ and 350 K to 2.65×10^{12} atom-pulse^{-1} cm^{-2} for F_0 and 450 K. In each case, the number of pulses was adjusted to reduce the Br coverage from 0.25 to 0.06 ML. This produced surfaces closely resembling Figs. 2(c) or 2(d).

The desorbing species in thermal[12,13] and laser[5,6] etching of GaAs surfaces are gallium mono- and trihalides and molecular arsenic for surfaces exposed to achieve submonolayer Cl or Br coverages. Halogen desorption is not observed at comparable laser intensities.[5] Hence, the partitioning of Br between $GaBr_3$ and GaBr desorption channels can be derived from the etch yield.[13] Since As desorbs without Br and the surface remains stoichiometric, the number of substrate atoms removed per Br atom is 2/3 for the $GaBr_3$ channel and 2 for the GaBr channel. The overall etch yield was 0.793 from Figs. 2(c) and 2(d) so that $\sim$90% of the Br was removed as $GaBr_3$. This emphasis on $GaBr_3$ is in sharp contrast with that for thermal etching. Although the thermal spike due to laser heating reaches 650–700 K, $GaBr_3$ desorption in thermal etching at these temperatures accounts for $<$10% of the Br consumption for similar initial coverages.[13] The difference reflects the concentration of Br in islands to facilitate $GaBr_3$ formation and activation afforded by the distribution of energetic carriers in photochemical effects.

To form a volatile $GaBr_3$ precursor from a structure like that depicted at the bottom of Fig. 2 requires that two Br atoms be inserted into Ga-As bonds. Presumably, the rate-limiting step consists of the formation of volatile $GaBr_3$ from a $GaBr_2$ transient state and a Br from a nearby site. The concentration of $GaBr_2$, converted photochemically from the original GaBr, should be proportional to the surface carrier density. And the probability of the final Br insertion, which can be expressed by an effective concentration of activated Br, should also be proportional to the surface carrier density. Since the surface carrier density is proportional to the laser intensity under our experimental conditions, we expect second-order kinetics in photon intensity. Fitting the yield data for 350 K to a power law for $F\leqslant13.5$ mJ cm^{-2} indeed gives an F^2 dependence. At higher intensities, however, the yield increases more rapidly, $F^{2.7\pm0.1}$ as thermal spikes become increasingly important. Corresponding treatment of the data at 450 K indicates an $F^{2.1}$ dependence at low intensity and $F^{2.8}$ dependence at higher intensities. For a given intensity, the desorption yield increases by a factor of 4 to 5 from 350 to 450 K.

Substrate-mediated charge-transfer is the dominant photochemical process for Br-GaAs(110) when the photon energy is 2.3 eV. For the starting surface with Br bonded to Ga and As, this energy is insufficient to excite the bonding orbitals or to induce direct bonding to antibonding transitions involving the adsorbates.[16] Photoabsorption in GaAs creates electron-hole pairs, and some of them can participate in etching if they are generated close enough to the surface. For nanosecond pulses with more than 1 mJ cm^{-2} per pulse, the density of photocarriers in the semiconductor depletion region exceeds the dopant concentration by orders of magnitude and the surface electronic system is far from equilibrium.[1,18] Most of these hot carriers lose energy in $\sim10^{-12}$ s by collisions with optical phonons. Recombination involving cold carriers usually occurs in a much longer time scale, $10^{-9}-10^{-7}$ s. Simple estimates show that for a 4.5 mJ cm^{-2} pulse, the number density of electron-hole pairs generated within 50 Å of the surface exceeds the substrate material removal by at least four orders of magnitude. Thus, the role of these band-edge carriers seems to be minimal. If we focus on the desorption yield for $F=4.5$ mJ cm^{-2} and $T_0=350$ K where thermal effects are minimal, each pulse delivers 1.2×10^{16} photons cm^{-2} and 2.2×10^9 atoms cm^{-2} are removed (Fig. 3). The yield of $\sim1.8\times10^{-7}$ atom-photon^{-1} deduced here compares favorably with a typical value of $10^{-7}-10^{-6}$ observed in laser-etching ($h\nu=2.4$ eV) of GaAs with gas-phase reactive Cl species (from a plasma discharge of HCl).[2]

Bromine insertion events on terraces should involve localization of a photogenerated hot hole between a Ga-As bond where the Br concentration is like the schematic in Fig. 2. They should also involve charge transfer to Ga-Br antibonding states. This initiates Br transfer from an adjacent As site, for example, to form $GaBr_2$(a) with two modified backbonds. This process is not likely to be exothermic and may require energetic photocarriers for activation. The formation of the intermediate $GaBr_2$(a) state alters the local atomic and electronic structure so that the second Br insertion follows a

different (and unknown) potential energy surface. This Br must be acquired from a nearby site on the same row or an adjacent row, possibly with coordinated motion involving As. The experimental dependence of the desorption yield on the square of the intensity is consistent with the scenario in which the formation/desorption of $GaBr_3$ is the rate-limiting step. This intuitive picture should apply to $GaBr_3$ formation for both terrace pit creation and expansion, though the latter will have different initial bonding configurations and Br transfer trajectories. Molecular-dynamic simulations with accurate potentials will be needed to evaluate the lifetime of transient $GaBr_2$(a) state and the insertion barriers.

The F^2 dependence of the yield suggests that $GaBr_3$ formation is the rate-limiting step. This requires that Br adatoms are able to move sufficiently so that the reaction is not limited by the sampling rate of the necessary precursors. This is plausible since pit initiation and expansion occur in Br islands. Moreover, the population of Br is high at pit edges since such sites are favorable adsorption sites.[12]

While the F^2 dependence of desorption yield at low laser intensity points to a photochemical reaction mechanism, it is also clear that thermal contributions increase with F and T_0. To estimate the contributions that would arise from pure thermal processes, we need the peak temperature and the overall barrier for the $GaBr_3$ channel. To calculate the maximum temperature rise ΔT_{max} and its duration τ at each laser pulse, we adopted the simplified one-dimensional heat diffusion model.[19,20] This model is valid when the laser spot size is much larger than the thermal diffusion length l_T during the pulse. The thickness d heated by a pulse of duration τ_{pulse} is then the larger of the optical-absorption length l_{opt} or the thermal diffusion length $l_T \approx (4D_T\tau_{pulse})^{1/2}$ where D_T is the thermal diffusivity. Hence,

$$\Delta T_{max} \approx F(1-R)/(\rho c d),$$

and

$$\tau_T \approx \tau_{pulse} + d^2/(4D_T),$$

where F is the pulse energy intensity (J cm^{-2}), R is the reflectivity, c is the specific heat (J K^{-1} g^{-3}), and ρ is the density (g cm^{-3}). This assumes that there are no optical inhomogeneities, that the optical and thermal properties are independent of temperature, and that there are no phase changes. The relevant parameters are $R=0.35$, $d \approx 5 \times 10^{-5}$ cm, $c=0.35$ J K^{-1} g^{-1}, $\rho=5.32$ g cm^{-3}, and $D_T = 0.24$ cm^{-2} s^{-1} (Ref. 21). Hence, $\Delta T_{max} \approx 300$ K and $\tau_T \approx 10$ ns for our maximum laser intensity F_0 (45 mJ cm^{-2}). This gives rise to a peak temperature that is sufficient to activate thermal desorption since the threshold for etching is $\sim$500 K (Ref. 13). For $0.3F_0$ (13.5 mJ cm^{-2}) at 350 K, however, the peak temperature reaches only $\sim$440 K and thermal etching is negligible. When applied to pulsed-laser heating of Si, the estimation from this simple one-dimensional (1D) model agreed pretty well with more elaborated methods based on numerically solving the heat transport equation using temperature-dependent thermal properties.[19,20] We estimated that the uncertainty in our temperature estimation is ± 50 K for the maximum laser intensity. As a check, we irradiated a cleaved GaAs(110) sample with pulses with doubled maximum intensity ($\sim$90 mJ cm^{-2}) by replacing the dispersive lens. This disrupted the surface such that no stable tunneling condition could be obtained in STM. Moreover, the irradiated part of the sample showed optical inhomogeneity when examined with an optical microscope. Since it is known that annealing GaAs(110) to $\sim$800 K leads to disruption of the surface with preferential evaporation of As and clustering of Ga[12] we inferred that our power-doubled beam caused a rise of at least 500 K. Accordingly, the surface temperature rise in our normal laser setting was at least 250 K. This value falls into the range 300 ± 50 K, as derived from the 1D heat transport model.

We can estimate the thermal contribution to desorption by assuming that it scales as $\exp(-E_a/k_BT)$, where E_a is the activation energy and T is the peak temperature. We used $E_a = 75$ kJ mol^{-1} derived from temperature-programmed desorption (TPD) experiments for $GaCl_3$ desorption.[22] To eliminate the pre-exponential factor, we normalized to the datum point at 45 mJ cm^{-2} and 450 K. This greatly overestimated the thermal contribution since it implied that etching was entirely due to heating, but it provided an upper limit for the thermal etching at lower intensities. From Fig. 3, direct thermal etching estimated in this way is negligible for $F \leq 13.5$ mJ cm^{-2} at 350 K. Similarly, it could account for less than 30% of the total at 450 K in the same intensity regime.[23] An alternate way of eliminating the pre-exponential factor would be to assume that all reaction is photochemical at $0.1F_0$ and extrapolate the F^2 relation to $F=F_0$ and attribute the difference to heating. This provides a lower bound for direct thermal desorption, indicating that direct thermal desorption accounts for more than 2/3 of the total yield at F_0 and 450 K.

The effect of photon polarization was examined by rotating the sample 90° around the incident beam so that we had $\mathbf{E} \| [1\bar{1}0]$ rather than $\mathbf{E} \perp [1\bar{1}0]$. In the etching regime, the desorption yield and the etch pit profiles showed no polarization dependence. Regardless of the polarization, pit initiation occurred randomly in areas where there were Br islands. The carriers participating in the photochemical reactions are three dimensional since the relevant transitions for 2.3 eV photons only involve those of bulk GaAs and these are insensitive to polarization. Transitions that might be dependent on polarization would include intrinsic surface states and the Ga-Br or As-Br levels. However, Br adsorption on the terraces suppresses the intrinsic surface states and the bonding-antibonding separations for Ga-Br and As-Br are too large to be accessible.

From these measurements, it is clear that photochemical processes account adequately for the low intensity results but that the yield increases at a rate that is higher than expected if only photochemical processes were playing a role. Moreover, thermal processes alone cannot account for the observed fourfold to fivefold increase in the desorption yield from 350 to 450 K in the low intensity regime. We conclude that the two effects that have been usually assumed (implicitly or explicitly) to function independently must be considered to be complementary. Our results demonstrate three regimes: desorption at low laser intensity driven almost entirely by photochemical processes, desorption at high laser intensity driven largely by thermal desorption, and desorption at intermediate intensities where photochemical and

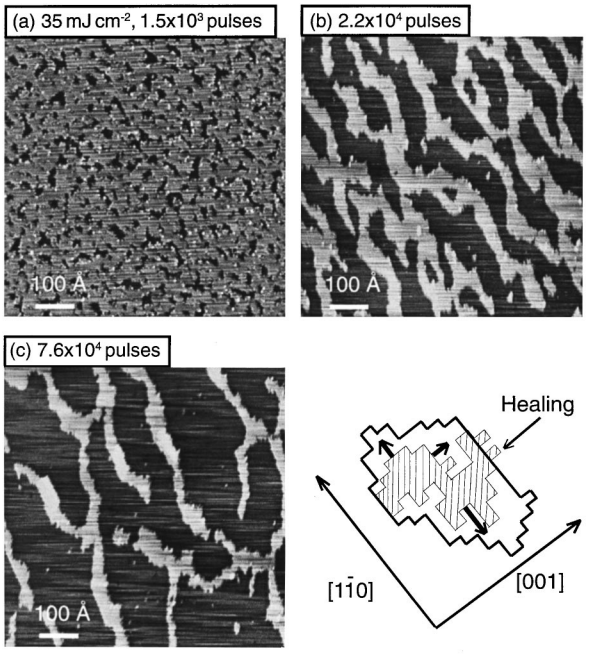

FIG. 4. Images that demonstrate laser-induced desorption of Ga and As from pit boundaries. The base temperature is 300 K. (a) Surface morphology after irradiation of a surface equivalent to Fig. 2(a) showing distributed pits of highly irregular shapes. The Br concentration is <2% at this stage. (b) Long vacancy strips are produced after higher irradiation because atom desorption favors pit growth along [110]. (c) The top layer shrinks further with increased irradiation but the yield decreases. Analysis shows the ratio of atoms on [110] steps to those across [110] approaches ~3.5:1. (d) Schematic showing pit growth that favors extension along [110]. The hatched area represents an irregular pit and the bold lines depict its shape after laser-induced desorption. Healing tends to eliminate kinks and leads to more regular steps. It also accounts for the observation of residual top layers which have lower defect densities than those produced by initial photoetching [750×750 Å^2].

thermal processes are intimately linked. By inference, models of photochemical processes should also consider the motion of surface atoms.

C. Laser-induced atom desorption: Etch-pit growth via electronic excitation

This section focuses on laser-induced desorption of Ga and As after terrace pitting has consumed the etchant. It is important to note that equivalent irradiation of clean surfaces has minimal effect. This process is analogous to desorption induced by electronic transition for gas-solid systems.[24] Here, we examine the dependence on crystallographic orientation, laser intensity, and temperature.

Figure 4 shows the evolving top layer morphology for a sample held at 300 K. To obtain Fig. 4(a), we irradiated a surface equivalent to Fig. 2(a) having 0.25 ML Br using 1.5×10^3 pulses at $F=35$ mJ cm^{-2}. This reduced the Br concentration to below 2% while creating etch pits that were highly irregular in appearance and accounted for 18% of the top layer (pit density 6×10^{12} cm^{-2}). The total step length was 3×10^6 cm/cm^2 and 0.17 ML of top-layer atoms were located in unit cells that bordered the pits. As depicted in Fig. 4(d), the numbers of cells on [110] steps and on steps that cross [$\bar{1}$10] are about equal. The step energy is very high for these photoetched surfaces, reflecting the highly nonequilibrium conditions for pit formation. Increasing the base temperature to 450 K during formation had little effect on the pit profiles in this etching stage. Apparently, the Br adatoms greatly hinder the diffusion of substrate atoms and vacancies that could lead to lower energy configurations. Surface healing does occur during prolonged irradiation after Br has been consumed.

Continued desorption evident from Fig. 4(b) causes pit expansion that occurs preferentially along [110]. This produces top layer stripes that have an average width of 53 Å along [001] and are separated by 65 Å gaps. Stripes represent 48% of the surface at this stage. The total step length was 1.3×10^6 cm/cm^2; unit cells defining the steps represent 0.10 ML. The incremental removal of 0.34 ML with 2.05×10^4 pulses gives a yield of 1.6×10^{-7} atom photon^{-1}. This is about two orders of magnitude lower than the photoetching yield at the same laser power (see Fig. 3). Expansion by pit growth along [110] increases the number of atoms on [110] steps. It can also reduce those on steps across [110] when pits overlap. Comparing Figs. 4(b) and 4(a) indicates that significant healing at pit boundaries has accompanied pit growth. Thus, the morphology in Fig. 4(b) does not correspond to simple expansion of the pits in Fig. 4(a) since this would give much thinner top layer strips. As depicted in Fig. 4(d), healing reduces pit irregularity by forming $\langle 11n\rangle$, $\langle 110\rangle$, and $\langle 001\rangle$ steps. Healing also accounts for diffusion of vacancies to larger pits. Overall, the ratio of unit cells along [110] versus across [110] has increased to 3:1, reflecting easy desorption of twofold-coordinated atoms on steps across [110].

Occasionally, cleaving produces steps that are oriented approximately along [110]. Double-height steps can be produced when etching into lower terraces occurs near such steps. These steps usually consist of {111} microfacets with periodic reconstructions. They are analogous to those produced by etching during continuous exposure to Br at 700–775 K[12] or after sputtering with 300–500 eV Ar ions in the same temperature range.[25] They have also been observed in growth at 715–725 K.[26] The consequences of their production in etching is that they pin the step by their higher stability.

Continued irradiation to produce Fig. 4(c) reduces the top layer without inducing defects in the newly exposed layer. The desorption yield 0.23 ML by 5.4×10^4 additional pulses decreased because of the smaller number of desorption sites and a smaller proportion of boundary units across [110]. Top-layer strips average 42 Å in width and are separated by 115 Å. The ratio of unit cells along and across [110] steps has increased only slightly to 3.5:1, despite a 50% reduction of the total step length from Fig. 4(b). This suggests that the desorption probability from a site on steps across [110] is three to four times as high as kink creation on [110]. In this regime, the removal rates for the two types of steps are such that their ratio on the surface has little dependence on irradiation time. Etch pits showed a comparable aspect ratio, ~4.5, in favor of elongation along [110] in continuous thermal etching at 725 K with low-flux Br_2.[12]

Laser-induced desorption is stoichiometric under our experimental conditions. While the terminating species on a

particular step segment usually are not equally distributed, there is an overall balance of Ga and As on a large scale throughout all stages. In addition, higher resolution images reveal that kink creation is as likely on Ga- and As-edged [110]. The fact that kink creation occurs but terrace pitting does not indicates a lower barrier for desorption from steps, though both involve the removal of threefold-coordinated atoms. Steps and other defect sites on semiconductor surfaces form sinks that can localize the excitation energy.[8]

As expected, the yield per pulse depends sensitively on the laser intensity. For example, it took 1.2×10^3 pulses at 45 mJ cm^{-2} to remove 0.11 ML at 300 K whereas it took 6×10^4 pulses to achieve the same effect at 13.5 mJ cm^{-2}, starting from surfaces with an initial pit area of 0.34 ML. This scaling as $F^{(3-3.5)}$ is comparable to what has been observed by measuring the Ga^0 emission from GaAs(110) for similar photon energies and pulse intensities.[8] We note that pitted surfaces like Figs. 4(a) and 4(b) showed no atom desorption when heated to 650 K for 20 min and that our maximum power would increase the surface temperature by ~300 K to only ~600 K. Hence, electronic excitations are the key ingredient in laser-induced desorption of GaAs(110).

Atom desorption initiated by electronic excitation can be described by the Menzel-Gomer-Redhead (MGR) model.[27] The basic ideas of this model have been applied successfully in many chemisorption systems.[24] Desorption is initiated by an (externally driven) Franck-Condon transition that excites the complex from the ground state onto an antibonding potential energy surface where nuclear separation adjusts to the electronic state. Desorption can occur if the adsorbate-surface separation reaches a critical distance in the absence of a transition to either the ground state or a suitable metastable state. In our case, adsorbates are replaced by defects represented by pit boundaries or cleavage steps. The experimental results demonstrate that these sites are vulnerable because they form sinks for localized electronic excitation and because of their weaker bonding. In this aspect, laser-induced desorption shows remarkable site selectivity, superior to inert ion sputtering[28] or keV electron bombardment.[29] This makes laser desorption a promising technique for layer-by-layer removal, in conjunction with various vacancy seeding techniques.[15]

The power-law dependence of the desorption yield on laser power could result from multiple electronic excitations and multiple bond breaking events. (Multiphoton ionization can be neglected since it requires peak laser intensities that are orders of magnitude higher than used here.[30]) Multiple electronic transitions are important if repetitive excitations occur within the relaxation time for the vibrations of surface atoms, 10^{-12} s.[31] The probability for such excitations can be calculated from the photon flux. The probability of finding n incident photons in a given time interval is $p_n=[N^n \exp(-N)]/n!$ if the average number is N [Ref. 32]. At $F=35$ mJ cm^{-2}, there are 9.4×10^{16} photons cm^{-2} per pulse (1.6×10^{13} photons cm^{-2} in an interval of 10^{-12} s). If the photoabsorption cross section is 10^{-18} cm^2 (Ref. 10) and the reflectivity is 0.35, then on average each site is excited $0.65\times(1.6\times10^{13})\times10^{-18}\approx10^{-5}$ times in an interval of 10^{-12} s. The probability for double excitation within 10^{-12} s is then $p_2\approx5\times10^{-11}$. This gives an accumulated probability of $\sim3\times10^{-7}$ for double excitation in the 6 ns duration of each pulse at $F=35$ mJ cm^{-2}. This compares with the quantum yield of 1.6×10^{-7} atoms photon^{-1}, from Figs. 4(a) and 4(b), where the density of available reaction sites is 10–17% of the total surface sites. The good accord between the estimated value and the experimental one indicates that multiple electronic excitations are important in the desorption.

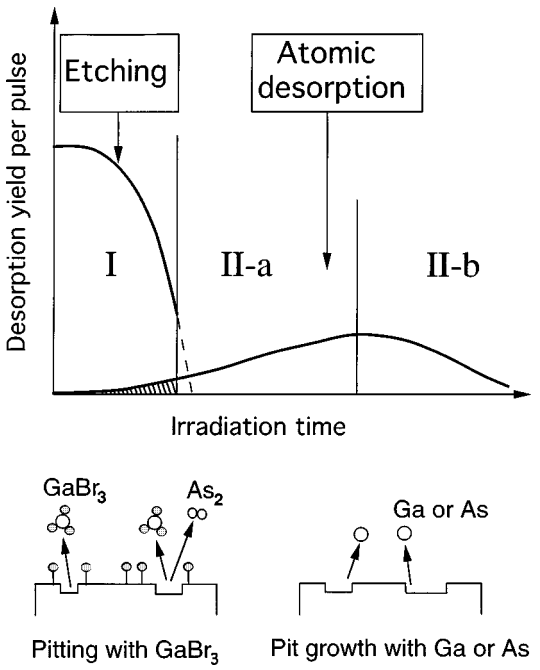

FIG. 5. Schematic of the yield per pulse. Initial irradiation creates and enlarges pits via Br etching (stage I). The desorption yield is high but it drops with the depletion of Br. Subsequent irradiation causes atomic desorption from pit edges (stage II). In this regime, the yield scales with the density of pit boundary atoms. This increases as individual pits grow (II-a) but it eventually decreases when pit overlap prevails (II-b). The hatched area in stage I shows that atom desorption is possible once pits are formed, though the yield is much smaller than for etching. The sketches suggest the dominant desorption products.

Since more than one surface bond must be broken for desorption to occur, the dependence of the yield on F should be more than the second-order dependence characteristic of double excitation pertinent to single bond breaking. Experimentally, we find an $F^{(3-3.5)}$ dependence which results from a combination of multiple electronic excitation and multiple bond breaking events. Theoretical calculations confirm that removal of less coordinated atoms costs less energy but do not support a direct proportionality between the number of bonds and the desorption energy barrier.[10]

Laser heating is expected to play a role in the desorption yield, as in photochemical etching discussed above. Indeed, the desorption yield increased by 50% when the base temperature was increased from 300 to 450 K for $F=13.5$ mJ cm^{-2} and it doubled from 9.2×10^{-5} ML between 300 and 450 K at 45 mJ cm^{-2}. At the maximum intensity, the peak temperature was enough that pit boundaries should be dynamic[13] and such atomic motion should facilitate desorption. On the other hand, direct thermal desorption at 45 mJ cm^{-2} should not be significant since it would result in nonstoichiometric changes on the surface. (Heating to ~800 K causes As evaporation and produces Ga clusters.[25]) The

above temperature dependence for atom desorption is much less than for laser etching where it was four to five-fold between 350 and 450 K. This difference should not be unexpected since removal of $GaBr_3$ and Ga^0 certainly involves different precursors and energy surfaces and temperature should have different effects on the relevant vibrational states.

IV. SUMMARY

The modification of Br-covered GaAs(110) is depicted in Fig. 5. In stage I, pits are created and Br is consumed, primarily through $GaBr_3$ desorption. Gallium loss is accompanied by desorption of molecular arsenic. The pits grow laterally due to Br etching, but the importance of etching diminishes as the Br is depleted. The pitted surfaces are highly irregular and their step density is very large. Thereafter, in stage II, pit growth occurs by atom desorption from pit boundaries. This laser-induced desorption has a yield that is about two orders of magnitude smaller than photoetching at the same laser intensity. The expanding pits first increase the number of sites that make up the steps but growth leads to pit overlap that reduces the step density. Laser-induced Ga and As desorption shows a clear crystallographic anisotropy that favors pit expansion in $[\bar{1}10]$ and stripe formation. Under our conditions, stoichiometric removal occurs during both photoetching and laser-induced atom desorption. Continued irradiation ultimately eliminates the residual top layer.[15]

This paper has shown the complementary nature of photochemical and photothermal effects in etching. Moreover, it has revealed the surface morphological consequences associated with these processes and laser-induced desorption. It has demonstrated that layer-by-layer removal is possible through laser-induced etching and atomic desorption. Multilayer planar removal can be achieved by alternatively roughening the surface using etching (or bombardment by energetic electrons or atoms) and then smoothing by laser-induced atomic desorption. The protocol presented here should have implications for semiconductor materials in general. Tuning the initial pit seeding and the photon energy will provide another dimension to surface patterning and material removal.

ACKNOWLEDGMENTS

We thank C. Y. Cha for contributions in the early stages of this work and Lin Huang, K. Nakayama, S. Jay Chey, and J. Kanasaki for stimulating discussions. This work was supported by the U.S. Army Research Office.

[1] See *Laser Microfabrication*, edited by D. J. Ehrlich and J. Y. Tsao (Academic, San Diego, 1989); T. J. Chuang, Surf. Sci. Rep. **3**, 1 (1983).

[2] C. I. H. Ashby, Appl. Phys. Lett. **45**, 892 (1984).

[3] A. W. Tucker and M. Birnbaum, Proc. SPIE Int. Soc. Opt. Eng. **385**, 131 (1983).

[4] F. A. Houle, Phys. Rev. Lett. **61**, 1871 (1988); Phys. Rev. B **39**, 10 120 (1989).

[5] G. Hasse, V. Liberman, and R. M. Osgood, Jr., J. Vac. Sci. Technol. B **10**, 206 (1992).

[6] M. Ishii, T. Meguro, T. Sugano, K. Gamo, and Y. Aoyagi, Appl. Surf. Sci. **79/80**, 104 (1994).

[7] K. Shudo, F. Komori, K. Hattori, and Y. Murata, Surf. Sci. **320**, 161 (1994).

[8] N. Itoh, J. Kanasaki, A. Okano, and Y. Nakai, Annu. Rev. Mater. Sci. **25**, 97 (1995); A. Okano, J. Kanasaki, Y. Nakai, and N. Itoh, J. Phys.: Condens. Matter **6**, 2697 (1994).

[9] J. Kanasaki, A. Okano, K. Ishikawa, Y. Nakai, and N. Itoh, Phys. Rev. Lett. **70**, 2495 (1993); K. Ishikawa, J. Kanasaki, Y. Nakai, and N. Itoh, Surf. Sci. **349**, L153 (1996).

[10] G. S. Khoo, N. Itoh, and C. K. Ong, J. Phys.: Condens. Matter **7**, 2051 (1995); N. Itoh, K. Hattori, Y. Nakai, J. Kanasaki, A. Okano, C. K. Ong, and G. S. Khoo, Appl. Phys. Lett. **60**, 3271 (1992).

[11] N. D. Spencer, P. J. Goddard, P. W. Davies, M. Kitson, and R. M. Lambert, J. Vac. Sci. Technol. A **1**, 1554 (1983).

[12] J. C. Patrin and J. H. Weaver, Phys. Rev. B **48**, 17 913 (1993); J. C. Patrin, Y. Z. Li, and J. H. Weaver, Appl. Phys. Lett. **62**, 1277 (1993); B. Y. Han, C. Y. Cha, and J. H. Weaver, Phys. Rev. B **56**, 4966 (1997).

[13] C. Y. Cha, J. Brake, B. Y. Han, D. W. Owens, and J. H. Weaver, J. Vac. Sci. Technol. B **15**, 605 (1997); J. Brake, C. Y. Cha, B. Y. Han, D. W. Owens, and J. H. Weaver, *ibid.* **15**, 670 (1997).

[14] J. L. Corkill and J. R. Chelikowsky, Phys. Rev. B **53**, 12 605 (1996); **50**, 11 924 (1994).

[15] C. Y. Cha, B. Y. Han, and J. H. Weaver, Surf. Sci. **381**, L636 (1997); B. Y. Han, C. Y. Cha, and J. H. Weaver, J. Vac. Sci. Technol. A **16**, 490 (1998).

[16] K. Cierocki, D. Troost, L. Koenders, and W. Monch, Surf. Sci. **264**, 92 (1992).

[17] The main criterion is that significant photoetching should have occurred but that the contribution of laser-induced desorption without Br should be minimal. This ensures good statistics in the data analysis.

[18] S. R. Morrison, *The Chemical Physics of Surfaces* (Plenum, New York, 1990).

[19] P. Baseri, S. U. Campisano, G. Foti, and E. Rimini, J. Appl. Phys. **50**, 788 (1979).

[20] J. Y. Tsao, S. T. Picraux, P. S. Peercy, and M. O. Thompson, in *Beam-Solid Interactions and Phase Transformations*, edited by H. Kurz, G. L. Olson, and J. M. Poate, MRS Symposia Proceedings No. **51**, (Materials Research Society, Pittsburgh, 1986), p. 283; C. I. H. Ashby and J. Y. Tsao, *Laser Microfabrication*, edited by D. J. Ehrlich and J. Y. Tsao (Academic, San Diego, 1989).

[21] S. M. Sze, *Physics of Semiconductor Devices* (Wiley, New York, 1969).

[22] C. L. French, W. S. Balch, and J. S. Foord, J. Phys.: Condens. Matter **3**, S351 (1991).

[23] This neglects the GaBr desorption channel because it has a higher barrier for desorption than $GaBr_3$. Inclusion would give a larger decrease for thermal contributions from F_0 to $0.3F_0$. The same conclusions regarding the dominance of nonthermal etching at low intensity can be obtained if E_a is taken to be 60–100 kJ mol^{-1} and ΔT is in the range 250–350 K.

[24] R. D. Ramsier and J. T. Yates, Jr., Surf. Sci. Rep. **12**, 243 (1991).

[25] X.-S. Wang, R. J. Pechman, and J. H. Weaver, J. Vac. Sci. Technol. B **13**, 2031 (1995).
[26] P. N. Fawcett, H. H. Neave, J. Zhang, and B. A. Joyce, Surf. Sci. **296**, 67 (1993).
[27] D. Menzel and R. Gomer, J. Chem. Phys. **41**, 3311 (1964); P. Redhead, Can. J. Phys. **42**, 886 (1964).
[28] E. Chason, P. Bedrossian, J. E. Houston, J. Y. Tsao, B. W. Dodson, and S. T. Picraux, Appl. Phys. Lett. **59**, 3533 (1991).
[29] K. Nakayama and J. H. Weaver (unpublished).
[30] *Multiphoton Ionization of Atoms*, edited by S. L. Chin and P. Lambropoulos (Academic, Orlando, 1984).
[31] J. A. Misewich, T. F. Heinz, and D. M. Newns, Phys. Rev. Lett. **68**, 3737 (1992).
[32] P. Meystre and M. Sargent III, *Elements of Quantum Optics* (Springer-Verlag, New York, 1991).